HNPS Advances in Nuclear Physics

Vol 31 (2025)

HNPS2024

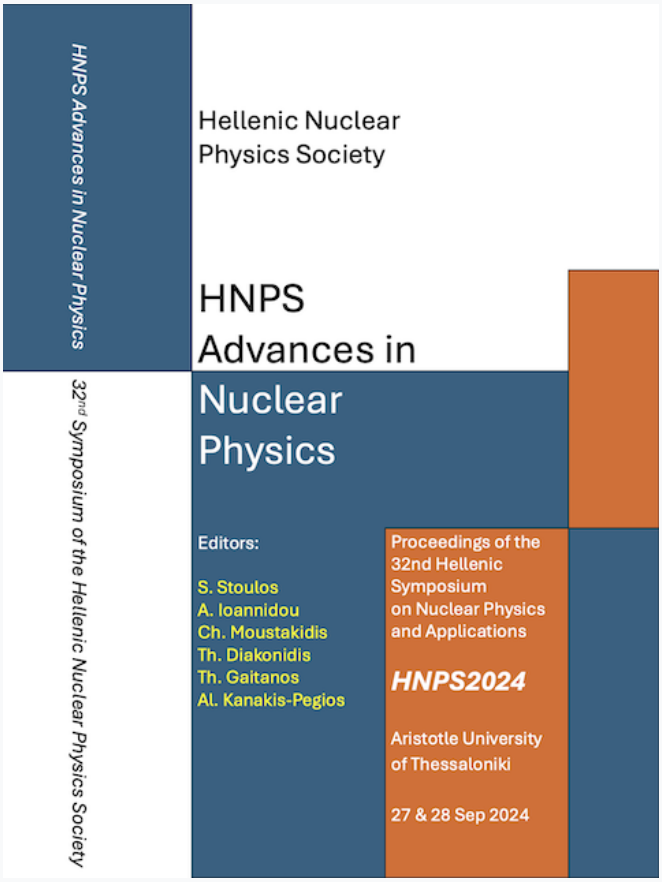

Reconstruction of radioactivity in semi-closed ocean systems using nuclear methods: a case study at North Cretan basin

Zoi Maniati, Christos Tsabaris, Effrosyni Androulakaki, Stylianos Alexakis, Kiki Manta, Dionisis Patiris, Michael Kokkoris

doi: 10.12681/hnpsanp.7998

To cite this article:

Maniati, Z., Tsabaris, C., Androulakaki, E., Alexakis, S., Manta, K., Patiris, D., & Kokkoris, M. (2025). Reconstruction of radioactivity in semi-closed ocean systems using nuclear methods: a case study at North Cretan basin. *HNPS Advances in Nuclear Physics*, *31*, 102–107. https://doi.org/10.12681/hnpsanp.7998

Reconstruction of radioactivity in semi-closed ocean systems using nuclear methods: a case study at North Cretan basin

Z. Maniati[1,2,*], C. Tsabaris[1], E.G. Androulakaki[1], S. Alexakis[1], K. Manta[1], D.L. Patiris[1], M. Kokkoris[2]

[1] *Hellenic Centre for Marine Research, Institute of Oceanography, 19013 Anavyssos, Greece*
[2] *National Technical University of Athens, Department of Physics, 5780 Athens, Greece*

Abstract A sediment core was collected using a box corer from the North Cretan deep basin, at a depth of 1500 m, in order to determine the rate of sedimentation, to measure the levels of radioactivity of ^{137}Cs and to investigate potential past geophysical events. The activity concentrations of the radionuclides were measured in the laboratory by the gamma spectroscopy method using a High-Purity Germanium (HPGe) detector at the Marine Environmental Laboratory of HCMR. The sedimentation rate was calculated applying radio-dating models by both the ^{210}Pb and the ^{137}Cs methods. The low sedimentation in the studied area exhibited folded peaks of the Cs deposition due to Chernobyl and nuclear tests. The results of the measurements showed that Cs appeared in the first 4 cm of the sediment core and its activity concentration ranged from (6.66 ± 0.62) Bq kg^{-1} to (1.39 ± 0.28) Bq kg^{-1}, with a value of (6.66 ± 0.62) Bq kg^{-1} on the surface sample. The sedimentation rate was estimated at (0.037 ± 0.007) cm y^{-1} with the ^{210}Pb radiochronology model. Additionally, it was observed the signature of the volcanic eruption that took place close to Santorini Island (almost 300 years ago) was evident at around 10.5-11.0 cm. The deep basin of the North Cretan Sea, although it does not interact with the terrestrial environment, was affected by anthropogenic pressures, as well as by the footprint of natural hazards.

Keywords HPGE, environmental radioactivity, sedimentation rate, gamma-spectrometry, radionuclides

INTRODUCTION

The deep ocean basins, as semi-closed systems, do not interact intensively with the atmosphere as well as with benthic oceanographic circulation of water masses. Thus, the deep ocean basins are considered valuable adequate laboratories for studying the cycle of key physicochemical magnitudes and tracers that play crucial role to the better understanding of the environmental processes and the ecosystem functioning [1-2]. The sediment is also a valuable marine matrix to study the evolution of any magnitude of interest (e.g. related discharged pollutants).

Due to increased technological activities since the onset of industrialization in the last century, several million tons of pollutants have been released into the environment, leaving a distinct stratigraphic signature in sediments. In recent years, significant efforts have been devoted to understanding the processes driving gradients in contaminant levels in response to changing climate conditions. One of the methods frequently applied, as described in the literature [3-5], involves reconstructing contaminant levels over the past century and correlating them with sedimentation/accumulation processes identified in sediment cores. The evaluation of long-term global geological processes, influenced by both natural and anthropogenic factors, is carried out using dating methods and appropriate "radio-clocks" [6]. In this context, considerable effort has recently been directed toward developing new methods for studying environmental microplastic pollution, incorporating radiotracers to better understand the behavior of chemicals and particles [7].

Recent research activities have focused on the reconstruction of marine environments in the deep basin of Lemnos in the North Aegean Sea [8], as well as in other marine regions, such as the Adriatic

* Corresponding author: zwhmaniath@gmail.com

and Black Seas. These studies aim to reconstruct radionuclide activity concentrations and analyze global change factors [5]. Temporal variations of key parameters were examined using sediment cores from deep-ocean environments to estimate sedimentation/accumulation rates and to assess any changes linked to climate. Sedimentation rates and chronology were determined using the ^{210}Pb dating method, validated by the ^{137}Cs method [3,5]. Regarding the Lemnos basin, it was found to be a semi-enclosed system that, despite its isolation, is influenced by anthropogenic activities through the advection of material from the northern part of Greece.

The aim of this work was to understand the phenomena occurring in the deep basin of North Crete, to study a semi-closed system and to assess the feasibility of applying radio-tracing techniques already implemented in these environments. However, significant information appeared in the core during the last five centuries. The activity concentrations of the natural and artificial radionuclides were analyzed to estimate the sedimentation rate in the study area. In this work, the sediment core was sampled in September 2020 from North Cretan basin. The core was sectioned into separate slices, and the natural and artificial radioactivity levels of each segment were measured using gamma spectroscopy. The measurements were performed using a calibrated High-Purity Germanium (HPGe) detector operated at the Marine Environmental radioactivity Laboratory of HCMR (MERL), which provided the vertical distribution of radionuclide activity concentrations. Using a dating model [3,5] based on lead ^{210}Pb and the ^{137}Cs radio-dating model, the sedimentation rate in this core was estimated separately for each method, and the vertical distribution of radionuclides in the sediment core was time-calibrated.

EXPERIMENTAL DETAILS

The sediment core was collected using a box corer from a depth of 1500 m at the coordinates 35°43'34.68"N, 25°7'50.52"E (Fig. 1). The Cretan basin, the southernmost part of the South Aegean, is bordered to the north by the shallow Cyclades Plateau (mean depth of roughly 200 m) and to the south by the island of Crete. It extends between 35°N and 37.5°N latitude and 23°E and 27.5°E longitude, covering an area of approximately 87,000 km². The basin is characterized by complex bathymetry, with depths ranging from 100 m to 2’500 m [9].

At the north part of the study area, there is a shallow submarine volcano called Kolumbo [10] (see Fig. 1), approximately 7 km northeast of Santorini Island [11]. In 1650 A.D., a volcanic eruption occurred, significantly affecting Santorini and the surrounding islands [12]. There slices of the core sediment samples in Cretan Sea provided new data in terms of radioactivity to better understand potential deposition mechanisms. According to the macroscopic description, a sedimentary volcanic origin was identified.

The sediment samples were prepared for measurement following IAEA standards [13]. The core was separated into samples of 1 cm-thickness, which were then dried in an oven at 50°C. The dried samples were weighed and grinded into a fine powder using an agate mortar. Subsequently, they were transferred into cylindrical plastic containers (6.8 cm in diameter, 1.9 cm in height), and the final mass of the sediment samples was calculated. Gamma-ray spectroscopy measurements were conducted using an HPGe detector (CANBERRA BE5030, diameter 101.6 mm, length 133.35 mm) with the appropriate electronic equipment (Digital Signal Analyzer, CANBERRA DSA-LX). The time measurement of each sample was 24 hours. To maximize the detection efficiency, the samples were positioned in close contact with the detector’s cover, optimizing the sample-to-crystal solid angle.

The analysis of all spectra was performed using SPECTRW software [14]. For the determination of activities, the photopeaks at 46 keV (^{210}Pb), 186 keV (^{226}Ra), 911 keV (^{228}Ac), 661 keV (^{137}Cs), and 609 keV (^{214}Bi) were used. The activity concentrations of the radionuclides ^{226}Ra, ^{228}Ac, ^{210}Pb$_{ex}$ and the anthropogenic cesium ^{137}Cs were determined. Appropriate correction factors for true coincidence summing (*TCS*) effects of simultaneously emitted gamma-rays and for sample self-absorption (*ET*), due

to differences in properties (density and composition) between the reference sources [15-16] and the samples, were calculated for each photopeak using the software EFFTRAN 4.5 [17]. The specific activity or activity concentration A (Bq kg^{-1}) for each radionuclide was determined using the following equation [18]:

$$A = \frac{cps}{eff \cdot m \cdot I_\gamma} \cdot TCS \cdot ET \quad (1)$$

where *cps* is the net count rate of each photopeak, calculated from the spectra, *eff* is the full energy peak efficiency of the sample, *m* is the mass of the sample and I_γ is the gamma-ray emission probability.

The sedimentation rate was determined using the ^{210}Pb dating method and the ^{137}Cs radio-dating model. For ^{210}Pb dating, the sedimentation rate was calculated based on the distribution of excess ^{210}Pb activity concentration ($^{210}Pb_{ex}$) using the Constant Flux: Constant Sedimentation (CF:CS) model [3,19]. This model assumes a consistent flux of $^{210}Pb_{ex}$ to the sediment surface and a constant sedimentation rate. The activity concentration A is expressed as a function of sediment depth (z) and sedimentation rate (v):

$$A(z) = A_o\, e^{\frac{-\lambda z}{v}} \rightarrow \ln A(z) = \ln A_o - \lambda \frac{z}{v} \quad (2)$$

where A_o is the activity concentration of $^{210}Pb_{ex}$ for z=0 and λ represents the decay constant.

The excess of $^{210}Pb_{ex}$ activity concentration in the samples was determined by subtracting the ^{214}Bi activity concentration from that of ^{210}Pb ($^{210}Pb_{ex}$ = ^{210}Pb - ^{214}Bi), under the assumption that ^{214}Bi and ^{226}Ra are in secular equilibrium since the sampled remained in the laboratory for about 20 days before the measurement process.

For ^{137}Cs dating, the method utilizes two characteristic peaks of maximum concentration within the sediment core. The first peak corresponds to 1963, reflecting the maximum concentrations in the air due to the nuclear fallout, while the second peak, dated to 1986, is associated with the Chernobyl accident. The identification of these ^{137}Cs peaks in each core enables the calculation of the average sedimentation rate, assuming a linear relationship between the peaks and depth. The mean sedimentation rates (v_i) after 1963 and 1986 are calculated, respectively:

$$v_i = \frac{z_i}{t_0 - t_i} \quad (3)$$

where t_0 is the date of the core extraction, t_i refers to 1963 or 1986 and z_i represents the corresponding sediment depth.

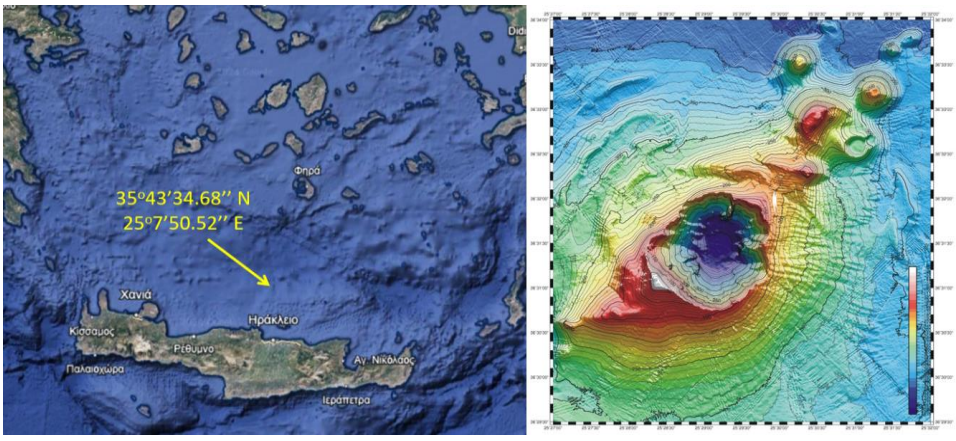

Figure 1. *Left picture: Sediment sampling position of North Cretan basin. Right picture: Kolumbo volcano [20]*

RESULTS AND DISCUSSION

As a first observation when opening the sediment core, volcanic tephra was observed at a depth of 9.5–11.5 cm. In this paragraph the activity concentration of radionuclides will be described. More specifically, the ^{226}Ra activity concentration ranges from (16 ± 1) Bq kg^{-1} to (33 ± 1) Bq kg^{-1}, of ^{228}Ac from (18 ± 1) Bq kg^{-1} to (39 ± 3) Bq kg^{-1} and ^{210}Pb$_{ex}$ from the minimum value that the detector can measure (MDA) [18] down to (279 ± 13) Bq kg^{-1} (Table 1). The activity concentration graphs for natural radionuclides, as a function of sediment depth, follow a similar pattern (Fig. 2). We observe that the graphs for ^{226}Ra and ^{228}Ac exhibit consistent behavior: their activity concentration increases within the first cm of the core, remains almost constant between 1.5 cm and 3.5 cm, rises again at 4.5–9.5 cm, decreases at 9.5–11.5 cm and stabilizes from 12.5 cm to 30.5 cm. The maximum activity concentration is observed at a depth of 9.5 cm. The activity concentration of excess ^{210}Pb decreases between 0.5 cm and 3.5 cm, remaining constant below this depth, except for a slight increase at 9.5–10.5 cm. The maximum activity concentration is observed at 0.5 cm (Fig. 3). As concerns artificial radioactivity, the activity concentration values for ^{137}Cs range from (1.39 ± 0.28) Bq kg^{-1} to (6.66 ± 0.62) Bq kg^{-1}, but the two peaks corresponding to nuclear fallout (1963) and the Chernobyl accident (1986) are indistinguishable (Fig. 3).

Using the ^{210}Pb dating method, the sedimentation rate was measured as v=(0.037 ± 0.007) cm y^{-1}. The value of the sedimentation rate taking into account the minimum value at the confidence interval within 1 sigma is 0.03 cm y^{-1} and it was selected for time-calibration according to the time marker of Kolumbo eruption as a reference point. The tephra from the eruption was primarily observed at a depth of 11 cm. Using v=0.03 cm y^{-1} and z=11 cm, the time between the eruption and the sampling date was calculated as t=367 y (by t=$\frac{z}{v}$). Thus, the experimental date of the Kolumbo eruption is 2020-367=1653, based on the ^{210}Pb radio-dating model. In case of the mean value of the sedimentation rate, the reproduced year is (1720 ± 60) years. This difference may probably come from the compaction factor of the sediment core since the studied system is very slow in terms of accumulation/sedimentation.

Using the ^{137}Cs radio-dating method, the sedimentation rate v=(0.021 ± 0.009) cm y^{-1} was calculated. For the ^{137}Cs model, it was assumed that the peak associated with the Chernobyl accident occurs at 0.5 cm and the peak for nuclear fallout at 1.5 cm depth, as no distinct energy peaks were observed in the graph. However, the Cs model is not effective since the system in terms of sedimentation/accumulation is very slow and the different Cs contributions are not distinguished.

The artificial radionuclide ^{137}Cs is hardly detected in sediments due to its low concentration, variable residence time in the water column and mobility within sediments caused by diffusion processes [9]. It should be noted that the diffusion model applied in this study is a simplification, and alternative approaches should be sought. The activity concentration of ^{137}Cs (above the minimum detectable activity, MDA) was observed at depths 2.5 cm and 3.5 cm. The presence of these peaks, which appear earlier than the timeline of nuclear weapon tests and the Chernobyl accident, suggests that diffusion of ^{137}Cs occurred along the sediment core depth. To study this phenomenon, the diffusion of ^{137}Cs was calculated for these four sediment layers of the core. The diffusion equation is [21]:

$$C = A \cdot e^{-\frac{z^2}{4 \cdot D \cdot \frac{z}{v}}} \quad (4)$$

where C is the activity concentration of ^{137}Cs (Bq kg^{-1}), A is the initial activity concentration of ^{137}Cs (Bq kg^{-1}) before diffusion, z is the depth of the core (cm), D is the diffusion rate factor (cm^2 y^{-1}) and the sedimentation rate v=(0.037 ± 0.007) cm y^{-1}. The factors A, D and coefficient of determination, R^2, were measured using the function y=a·e$^{b \cdot x}$, as shown in Fig. 3, with values of (7.65 ± 1.91) Bq kg^{-1}, (0.016 ± 0.005) cm^2 y^{-1} and 0.86, respectively. The diffusion model used in this work should provide better results if the ^{137}Cs data were made in a better depth resolution.

CONCLUSIONS

In this work, naturally occurring and anthropogenic radionuclides were studied in a sediment core from the Cretan deep basin 25 miles northern from Heraklion port, Crete. The sedimentation rate was estimated mainly using the ^{210}Pb dating model, assuming that the flux of ^{210}Pb$_{ex}$ to the sediment surface

Table 1. *Table of activity concentration values of ^{226}Ra, ^{228}Ac, ^{210}Pb$_{ex}$ and ^{137}Cs*

Radionuclide	Range of activity concentration (Bq kg^{-1})
^{226}Ra	(16 ± 1) - (33 ± 1)
^{228}Ac	(18 ± 1) - (39 ± 3)
^{210}Pb$_{ex}$	from MDA - (279 ± 13)
^{137}Cs	(1.39 ± 0.28) - (6.66 ± 0.62)

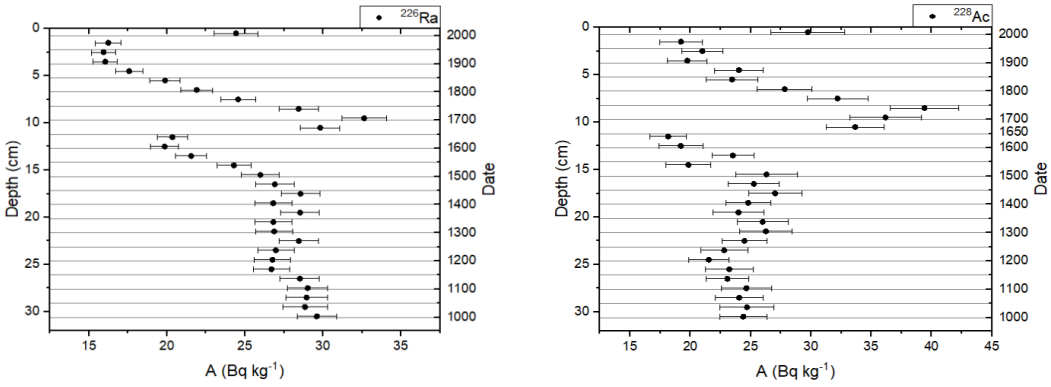

Figure 2. *The activity concentration distribution of ^{226}Ra and ^{228}Ac as a function of core depth*

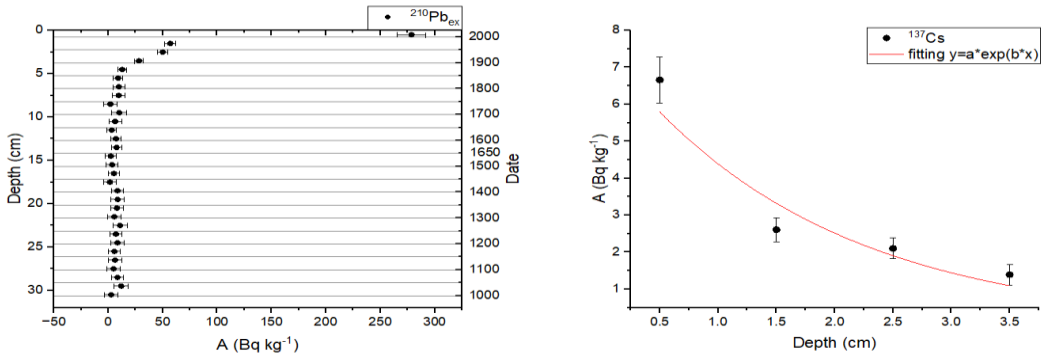

Figure 3. *Left picture: The activity concentration distribution of ^{210}Pb$_{ex}$ as a function of core depth. Right picture: Graph of the diffusion of radionuclide ^{137}Cs.*

and sedimentation rate remain constant. Additionally, the ^{137}Cs dating method is not adequate to be exploited as a radiotracer for dating purposes due to the very slow accumulation rate of material in the Cretan basin system (~0.03 cm y^{-1}). Vertical mobility of ^{137}Cs within the sediment core was observed and the diffusion rate factor was determined. The time marked of the Kolumbo eruption was identified by a distinct color change in the core at a depth of 11 cm. However, the maximum activity concentration of radionuclides was observed at a depth of 9.5 cm. Following the eruption, the volcanic plume and tephra were dispersed into the atmosphere, with their subsequent delayed deposition to the Cretan Sea and subsequently to the deep part of the deep basin at 1500 m. Further investigation is planned to measure chemical substance to identify the different deposition processes through the atmosphere and/or to the marine system reaching the seabed of the deep basin.

Acknowledgments

This work was supported by the MARRE project through National Strategic Reference Framework (NSRF) 2014–2020 co-financed by Greece and the European Union (European Social Fund ESF). The authors would also want to acknowledge the crew of the research vessel R/V AEGEAO for the sampling using the box corer during the cruise in the frame of MARRE project. The HCMR group would like also to acknowledge IAEA (RER7015 project) due to know-how transfer in terms of reconstruction of environmental magnitudes as well as the EU Horizon project with the acronym CONTRAST supporting updated tools for interpreting signatures from anthropogenic and natural processes using sediment cores.

References

[1] J. Liu, et al., J. Hazard. Mater. 487, 137101 (2025); doi: org/10.1016/j.jhazmat.2025.137101
[2] G. Kousidou et al., HNPS Adv. Nucl. Phys. 31, 96 (2025); doi: org/10.12681/hnpsanp.7999
[3] F.K. Pappa, et. al., Environ. Sci. Pollut. Res. 25, 30084 (2018); doi: 10.1007/s11356-018-2984-0
[4] F.K. Pappa, et al., Appl. Radiat. Isot. 145, 198 (2019); doi: 10.1016/j.apradiso.2018.12.021
[5] A. Vinković, et al., JSS 22, 2912 (2022); doi: 10.1007/s11368-022-03282-0.
[6] G. Eleftheriou, et al., HNPS Adv. Nucl. Phys. 21, 156 (2019); doi: 10.12681/hnps.2023
[7] C. Tsabaris, et al., J. Env. Rad. 144, 1 (2015); doi: 10.1016/j.jenvrad.2015.02.009
[8] C. Tsabaris, et al., JSS 24, 3938 (2024); doi: 10.1007/s11368-024-03907-6
[9] D. Kassis, et al., Ocean Dyn. 66, 11 (2016); doi: 10.1007/s10236-016-0987-2.
[10] A. Katsigera, et al., GeoHazards 5, 816 (2024); doi: org/10.3390/geohazards503004.
[11] P. Nomikou, et al., Glob. Planet. Change 90–91, 135 (2012); doi: 10.1016/j.gloplacha.2012.01.001.
[12] P. Nomikou, et al., ZfG 57, 029 (2013); doi: 10.1127/0372-8854/2013/S-00142.
[13] International Atomic Energy Agency, Guidelines on Soil and Vegetation Sampling for Radiological Monitoring, Technical Reports Series No. 486 (2019); ISBN: 978-92-0-102218-9.
[14] C.A. Kalfas, et al., Nucl. Instrum. Meth. Phys. Res. A 830, 265 (2016); doi: 10.1016/j.nima.2016.05.098.
[15] M. Alexander, J. Simon, M. Khanh Pham, Certified Reference Material IAEA-385: Natural and artificial radionuclides in sediment from the Irish Sea, International Atomic Energy Agency Department of Nuclear Sciences and Applications, Environment Laboratories, (2019); https://nucleus.iaea.org/sites/AnalyticalReferenceMaterials/Shared%20Documents/ReferenceMaterials/Radionuclides/IAEA-385/RS_IAEA-385_V5.3.pdf
[16] M. K. Pham, J. A. Sanchez-Cabeza, P. P. Povinec, Report on the worldwide intercomparison exercise: IAEA-385 radionuclides in Irish Sea sediment, International Atomic Energy Agency, Marine Environment Laboratory, (2005); https://nucleus.iaea.org/sites/AnalyticalReferenceMaterials/Shared%20Documents/ReferenceMaterials/Radionuclides/IAEA-385/IAEA_AL_151.pdf
[17] T. Vidmar, Nucl. Instrum. Meth. Phys. Res. A 550, 603 (2005); doi: 10.1016/j.nima.2005.05.055
[18] G. Eleftheriou, et al., Appl. Radiat. Isot. 206, 111234 (2024); doi: 10.1016/j.apradiso.2024.111234
[19] J.A. Sanchez-Cabeza, A.C. Ruiz-Fernández, Geochim. Cosmochim. Acta 82, 183 (2012); doi: 10.1016/j.gca.2010.12.024
[20] M. Klaver, et al., Geochem. geophys. 17, 3254 (2016); doi: 10.1002/2016GC006398
[21] N. Iversen, B. B. Jørgensen, Geochim. Cosmochim. Acta 57, 571 (1993); doi: 10.1016/0016-7037(93)90368-7